

Measuring the Transverse Velocity of Strongly Lensed Gravitational Wave Sources with Ground Based Detectors

JOHAN SAMSING,¹ LORENZ ZWICK,¹ PANKAJ SAINI,¹ DANIEL J. D'ORAZIO,^{2,1} KAI HENDRIKS,¹ JOSE MARÍA EZQUIAGA,¹ RICO K. L. LO,¹ LUKE VUJEVA,¹ GEORGI D. RADEV,³ AND YAN YU³

¹*Niels Bohr International Academy, The Niels Bohr Institute, Blegdamsvej 17, DK-2100, Copenhagen, Denmark*

²*Space Telescope Science Institute, 3700 San Martin Drive, Baltimore , MD 21*

³*The Niels Bohr Institute, Blegdamsvej 17, DK-2100, Copenhagen, Denmark*

(Dated: December 19, 2024)

ABSTRACT

Observations of strongly gravitationally lensed gravitational wave (GW) sources provide a unique opportunity for constraining their transverse motion, which otherwise is exceedingly hard for GW mergers in general. Strong lensing makes this possible when two or more images of the lensed GW source are observed, as each image essentially allows the observer to see the GW source from different directional lines-of-sight. If the GW source is moving relative to the lens and observer, the observed GW signal from one image will therefore generally appear blue- or redshifted compared to GW signal from the other image. This velocity induced differential Doppler shift gives rise to an observable GW phase shift between the GW signals from the different images, which provides a rare glimpse into the relative motion of GW sources and their host environment across redshift. We illustrate that detecting such GW phase shifts is within reach of next-generation ground-based detectors such as Einstein Telescope, that is expected to detect \sim hundreds of lensed GW mergers per year. This opens up completely new ways of inferring the environment of GW sources, as well as studying cosmological velocity flows across redshift.

1. INTRODUCTION

Binary black hole (BBH) mergers have been observed through their emission of gravitational waves (GWs) (Abbott et al. 2023), and their diversity in both masses (Abbott et al. 2019a, 2020), spins (Zackay et al. 2019; García-Bellido et al. 2021), and possibly eccentricity (Abbott et al. 2019b; Romero-Shaw et al. 2021a; Gayathri et al. 2022; Romero-Shaw et al. 2022; The LIGO Scientific Collaboration et al. 2023; Gupte et al. 2024) indicate that they form in various ways and astrophysical environments. Although several formation channels have been proposed, including dense stellar clusters (Portegies Zwart & McMillan 2000; Lee et al. 2010; Banerjee et al. 2010; Tanikawa 2013; Bae et al. 2014; Rodriguez et al. 2015; Ramirez-Ruiz et al. 2015; Rodriguez et al. 2016a,b,b; Askar et al. 2017; Park et al. 2017; Samsing 2018; Samsing & D'Orazio 2018; Samsing et al. 2020; Trani et al. 2021, 2022), isolated binary stars (Dominik et al. 2012, 2013, 2015; Belczynski et al. 2016b,a; Silsbee & Tremaine 2017; Murguia-Berthier et al. 2017; Rodriguez & Antonini 2018; Schröder et al. 2018; Iorio et al. 2023), hierarchical systems (Naoz et al. 2013; Li et al. 2014; Antonini et al. 2016; Antognini & Thompson 2016; Silsbee & Tremaine 2017; Randall & Xianyu 2018; Hamers & Thompson 2019; Martinez et al. 2020; Liu & Lai 2021; Trani et al. 2022), active galactic nuclei

(AGN) discs (Bartos et al. 2017; Stone et al. 2017; McKernan et al. 2017; Tagawa et al. 2020; Samsing et al. 2022; Trani et al. 2023; Fabj & Samsing 2024; Rom et al. 2024), galactic nuclei (GN) (O’Leary et al. 2009; Hong & Lee 2015; VanLandingham et al. 2016; Antonini & Rasio 2016; Stephan et al. 2016; Hoang et al. 2018; Hamers et al. 2018; Trani et al. 2019; Liu et al. 2019a; Liu & Lai 2021; Atallah et al. 2023), very massive stellar mergers (Loeb 2016; Woosley 2016; Janiuk et al. 2017; D’Orazio & Loeb 2018), and single-single GW captures of primordial black holes (Bird et al. 2016; Cholis et al. 2016; Sasaki et al. 2016; Carr et al. 2016), \sim 10 years of GW observations have not yet provided any clear picture of how each of these channels contribute to the observed merger rate, or if other channels need to be invoked to describe the observe properties (e.g. Zevin et al. 2021b).

There are reasons to believe that a large set of observations would help us constrain the underlying distributions of formation channels, as several key observables are likely to differ, e.g., dynamical systems will have distributions of random BH spins (e.g. Kalogera 2000; Rodriguez et al. 2016c; Liu & Lai 2018) and a subset of eccentric mergers (e.g. Gültekin et al. 2006; Samsing et al. 2014; Samsing & Ramirez-Ruiz 2017; Samsing & Ilan 2018; Samsing et al. 2018b; Samsing 2018; Samsing et al. 2018a; Samsing & D’Orazio 2018; Ro-

driguez et al. 2018; Liu et al. 2019b; Zevin et al. 2019; Samsing et al. 2019, 2020; Zevin et al. 2021a) with distinct distributions in LIGO-Virgo-KAGRA (LVK) (Samsing 2018), DECIGO/TianQin/Taiji (e.g. Chen & Amaro-Seoane 2017; Samsing et al. 2020), and LISA (Breivik et al. 2016; Samsing & D’Orazio 2018; D’Orazio & Samsing 2018; Kremer et al. 2019), whereas binary stars are likely to create BBH mergers with correlated spins on near-circular orbits. However, even constraining sub-channels within the dynamical channel is difficult. For example, eccentric BBH mergers are expected in both globular clusters (GCs) (e.g. Samsing 2018), galactic nuclei (GN) (e.g. O’Leary et al. 2009), active galactic nuclei (AGNs) disks (e.g. Samsing et al. 2022; Fabj & Samsing 2024), and through Lidov-Kozai oscillations in hierarchical multiple BH stellar systems (e.g. Hoang et al. 2018; Liu et al. 2019b; Liu & Lai 2021), although these channels are of completely different nature.

These challenges have led to ideas on how to probe the origin and assembly mechanism of individual BBH mergers case-by-case (e.g. Barausse et al. 2014; Meiron et al. 2017; Zwick et al. 2023; Samsing et al. 2024), with the idea of looking for features or imprints in the GW form that can tell something about the nearby environment. For example, if the BBH evolves in a gaseous medium, the BHs will experience extra drag-forces, which will show up as a change in the GW frequency evolution that is different from General Relativity (GR) (e.g. Barausse et al. 2014; Garg et al. 2022; Zwick et al. 2023). One can also probe the acceleration of the center-of-mass (COM) of the BBH as it spirals in (e.g. Yunes et al. 2011; Inayoshi et al. 2017; Robson et al. 2018; Chamberlain et al. 2019; Randall & Xianyu 2019; Wong et al. 2019; Tamanini et al. 2020; D’Orazio & Loeb 2020; Toubiana et al. 2021; Strokov et al. 2022; Xuan et al. 2023; Laeuger et al. 2023; Vijaykumar et al. 2023; Tiwari et al. 2024), which can be linked to the surrounding gravitational field, and even the dynamical formation pathway leading to merger (Samsing et al. 2024; Hendriks et al. 2024a,b). Modulations to the GW waveform could also hint for new physics, help constraining dark matter properties, or other exotic phenomena.

In this paper we explore how the relative proper (transverse) velocity of BBH mergers can be constrained in strong gravitationally lensed systems, where two or more images of the GW source are observed. When the wavelength of the GW emission is significantly smaller than the characteristic size of the lens, gravitational wave lensing and the lensing of light are expected to behave nearly identically in the geometric optics limit (see e.g. Ezquiaga et al. 2021). Although the first detection of strongly lensed GWs is expected in the coming years (Abbott et al. 2021, 2024), the full power of GW lensing will come in the era of Einstein Telescope (ET) and Cosmic Explorer (CE), when one expects to see \sim hundreds of strongly lensed events per year (e.g. Xu et al. 2022; Smith

et al. 2023). This has sparked an enormous recent interest and early searches (e.g. Dai et al. 2020) with implications for probing dark matter sub-structures (Tambalo et al. 2023; Çalışkan et al. 2023), wave optics (Takahashi & Nakamura 2003; Tambalo et al. 2023; Savastano et al. 2024), cosmology (Cremonese et al. 2021; Jana et al. 2023; Chen et al. 2024), strong fields (Gondán & Kocsis 2022; Pijnenburg et al. 2024), and modified gravity (Ezquiaga & Zumalacárregui 2020; Goyal et al. 2021, 2023).

The reason why two or more images of strongly lensed GW source allow for a measure of (transverse) velocity is that the images essentially define different lines-of-sight towards the BBH from the observer (see Fig. 1). This implies that any non-zero velocity of the GW source relative to the gravitational lens and the observer will project differently along the different lines-of-sight, and will therefore show up as GW images with slightly different Doppler shifts (e.g. Itoh et al. 2009; Savastano et al. 2024). The relative Doppler shift between pairwise images can be inferred by comparing their GW phase evolution, and the resultant GW phase shift can therefore be mapped to the relative transverse velocity between the observer, lens and GW source system.

As we here focus on cosmological strongly lensed systems, the relative velocity of the GW source will have components from its own motion inside its host galaxy, the motion of the galaxy within its environment, e.g. a galaxy cluster, and this environment relative to the cosmic flow. The contribution from each of these components depend on the redshift, host galaxy type, and generally the cosmological environment from local to cosmic scales; e.g., a typical galaxy has an internal velocity dispersion $\sigma \sim 100 \text{ km s}^{-1}$, the Milky Way is part of a small local group with a $\sigma \sim 60 \text{ km s}^{-1}$, where galaxies in the large COMA cluster have $\sigma \sim 1000 \text{ km s}^{-1}$. The idea of using strong lensing to probe relative (transverse) motions across the universe is therefore also a probe of the cosmic flow, how it depends on galaxy types, and how these correlate with the production of GW sources. We therefore envision this to also be an interesting and independent probe of cosmological dynamics using GWs in addition to other methods (e.g. Fishbach et al. 2018; Farr et al. 2019; Romero-Shaw et al. 2021b; Ezquiaga & Holz 2022; van Son et al. 2022; Biscoveanu et al. 2022; Fishbach & Fragione 2023). In terms of GW science, the particular interesting question is if the formation of GW sources are correlated with a particular galaxy or cluster type that can be constrained through their cosmic flow.

With three or more strongly lensed images, the direction of the relative transverse velocity vector can be triangulated, and we will therefore occasionally refer to this method as *Doppler Triangulation*. Variations of this method and moving lens effects in general have been discussed on several occasions in the literature, both in terms of electromagnetic signals (Kayser

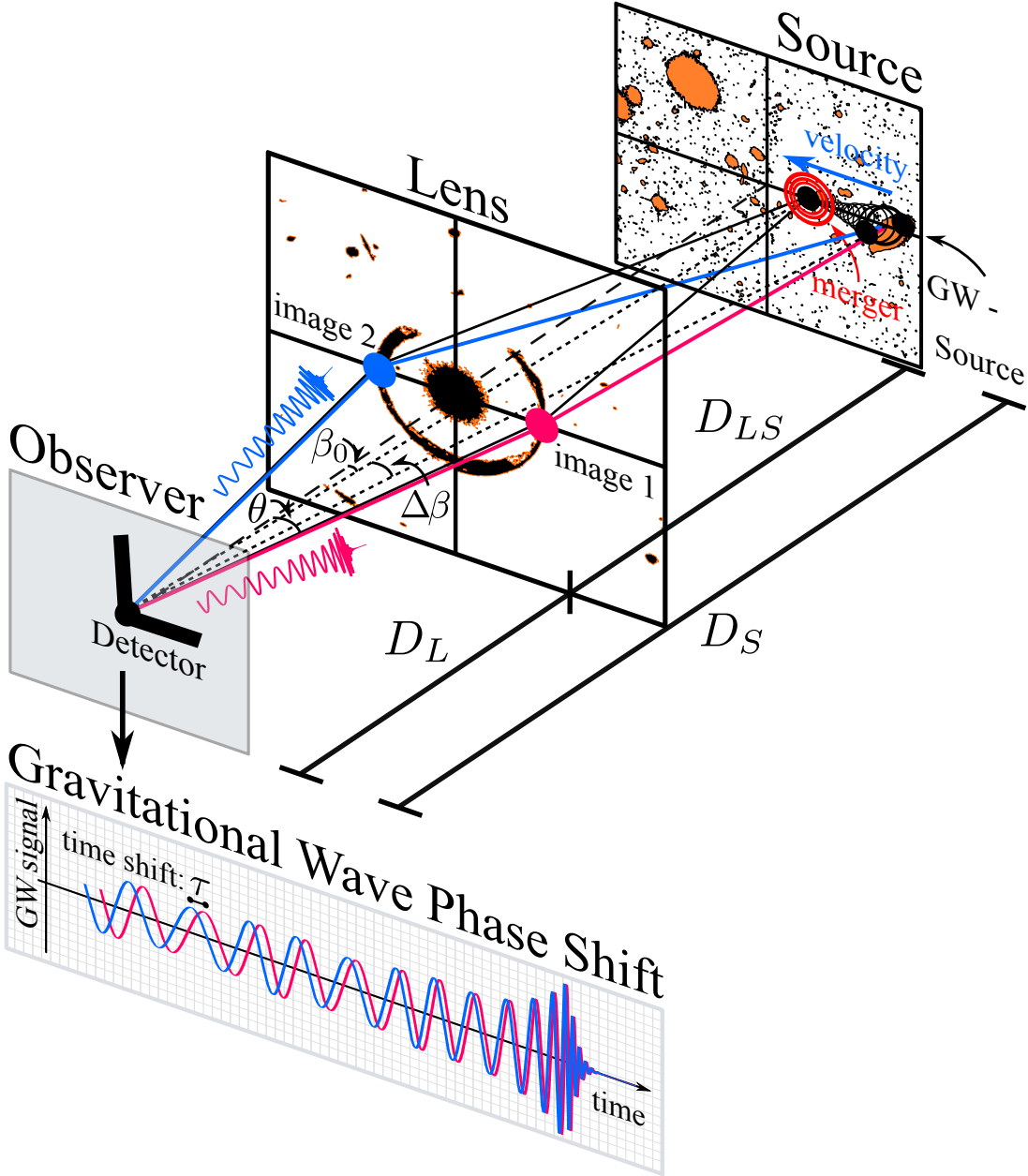


Figure 1. Illustration of a Strongly Lensed moving Gravitational Wave Source. The *Top Panel* of the figure shows our considered Observer-Lens-Source setup, with the detector in the *Observer*-plane, the gravitational lens in the *Lens*-plane, and the lensed GW source in the *Source*-plane. In this illustration the GW source is moving in the source plane, which takes it from an angle $\beta = \beta_0 + \Delta\beta$ to the point of merger at β_0 . The transverse velocity vector of the GW source has different projected velocity components along the lines-of-sight toward the observer, which results in a differential Doppler shift between *image 1* and *image 2*. For GW sources, this will show up as a GW phase shift as illustrated in the *Bottom Panel*. The detectability for Einstein Telescope is shown in Fig. 4.

et al. 1986; Chitre & Saslaw 1989; Birkinshaw 1989; Wucknitz & Sperhake 2004), as well as for GW systems (e.g. Itoh et al. 2009; D’Orazio & Loeb 2020; Gondán & Kocsis 2022; Yang et al. 2024; Savastano et al. 2024) with implications for deci-hertz detectors such as DECIGO/TianQin/Taiji (Kawamura et al. 2011; Luo et al. 2016; Hu & Wu 2017; Liu et al. 2020). In this work we quantify and explore the possibilities for the upcoming next-generation ground-based detector ET,

which is expected to see \sim hundreds of lensed GW sources per year (e.g. Xu et al. 2022).

The paper is organized as follows. In Sec. 2 derive the basic relations for how a relative velocity between observer, lens, and source relates to a GW phase shift in the frame of the observer. In Sec. 3 we quantify the measurability of this GW phase shift for different lensing setups and source properties, through Signal-to-Noise ratio (SNR) calculations assuming

an instrument similar to the proposed ET. We conclude in Sec. 4.

2. MEASURING TRANSVERSE VELOCITY

Strong lensing of GW sources makes it possible to put constraints on the relative (transverse) velocity of the source, as each lensed image essentially allow the observer to see the GW source from different lines-of-sight (Itoh et al. 2009). If the GW source is moving relative to the lens and the observer, the different images will show different Doppler shifts, which can be used to triangulate for the velocity vector of the source. For example, in a static flat Universe, the difference in projected radial velocity, Δv , between two lensed images separated by a total angle 2θ is to leading order

$$\Delta v \approx 2\theta v, \quad (1)$$

where v is the transverse velocity of the GW source relative to the lens and observer (see Fig. 1). This gives rise to a differential Doppler shift, $\sim \Delta v/c$, that can be linked to a displacement in angular phase of the received GW signals, i.e. a GW phase shift, $\delta\phi$, that can be expressed as,

$$\delta\phi \approx 2\pi f t \Delta v / c \approx 4\pi \theta f t v / c, \quad (2)$$

where f and t is the GW frequency and time, respectively. The observable GW phase shift between images can therefore be used to infer the relative transverse velocity of the source, if enough cycles can be build up during the observation through the time t and GW frequency f .

In the following we describe the components that go into measuring the relative transverse velocity of the GW source in an expanding flat Universe assuming two images, with three or more following trivially. Throughout the paper we assume the thin-lens approximation, the geometric optics approximation, we describe the GW source as a point source, and generally assume a simple lens system that only leads to smooth changes as the source, lens and observer are moving relative to each other.

2.1. Relative Velocities in an Expanding Universe

The relative Doppler shift between the images that makes Doppler Triangulation possible, is not just sensitive to the motion of the source in the source plane, but depends generally on the relative velocity between the observer (O), lens (L) and source (S) (see Fig. 1). Similar effects will therefore also be seen if the lens moves and the source is at rest, which is a configuration that often is referred to as the moving lens effect (e.g. Yang et al. 2024). This effect has a particular interest for cosmic-microwave-background (CMB) experiments for e.g. probing the large-scale transverse velocity field (e.g. Hotinli et al. 2021; Beheshti et al. 2024). Below we derive and illustrate how the observer, lens, and source velocities combine in an expanding universe into an effective velocity.

In our setup we consider three planes denoted the *Observer plane*, the *Lens plane*, and the *Source plane*, as shown in Fig.

1. In an expanding universe, the relative velocities translate non-trivially between these planes, as measures of time and length scale with the expansion, or redshift, z . In the following we will project the different velocity contributions from the planes into an effective velocity of the source in the source plane, relative to the lens and the observer. For this we start by defining the transverse velocities in each plane as,

$$v_s = \frac{ds_s}{dt_s}, \quad v_L = \frac{ds_L}{dt_L}, \quad v_O = \frac{ds_O}{dt_O}. \quad (3)$$

where ds and dt denote transverse length- and time-differentials, and the subscripts ‘S’, ‘L’, and ‘O’ refer to the source, lens and observer planes, respectively. To translate these velocities into an effective velocity of the source in the source plane, we now consider the following projections of the length differentials onto the source plane (e.g. Kayser et al. 1986),

$$ds'_L = -\frac{D_S}{D_L} ds_L, \quad ds'_O = \frac{D_{LS}}{(1+z_L)D_L} ds_O, \quad (4)$$

where the super-script (‘ $'$) denotes that the (unprimed) quantity has been mapped to the source plane, D is the angular diameter distance, and z is the redshift. Similarly, time differentials projected onto the source plane are,

$$dt'_L = -\frac{1+z_L}{1+z_S} dt_S, \quad dt'_O = \frac{1}{1+z_S} dt_O. \quad (5)$$

By combining these differentials, one can now define an effective transverse velocity,

$$v' = v_S - \frac{1+z_S}{1+z_L} \frac{D_S}{D_L} v_L + \frac{1+z_S}{1+z_L} \frac{D_{LS}}{D_L} v_O, \quad (6)$$

which can be considered as the velocity of the source relative to a setup with lens and observer being fixed. Below we continue by illustrating how this effective velocity, v' , of the source in the source plane can be turned into an observable GW phase shift.

2.2. Gravitational Wave Phase Shift

Consider two GW signals that have been observed in a strong lensing event and subsequently being aligned such that their time of merger coincides (see Fig. 1). If one signal is Doppler shifted relative to the other, the two signals will show increasingly larger temporal displacement from each other when going backwards in time from the point of merger. If we denote this time displacement by τ at a given GW frequency f defined in the observer frame, then the GW phase shift can be approximated by,

$$\delta\phi = 2\pi\tau/T = 2\pi f\tau, \quad (7)$$

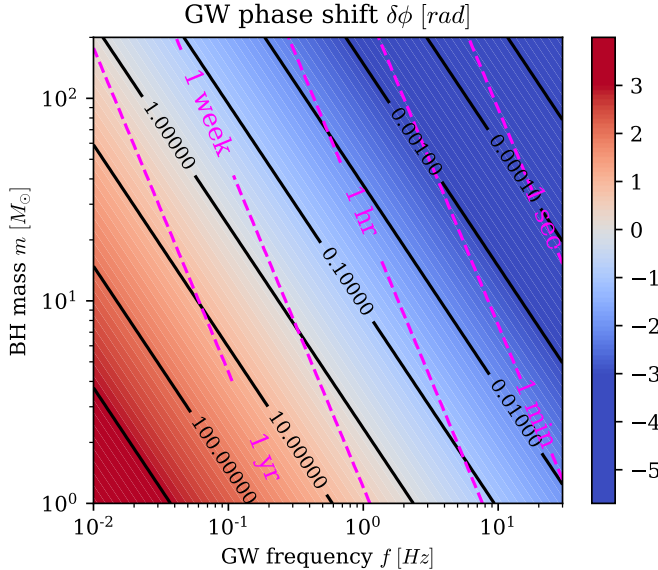


Figure 2. GW Phase Shift from Strongly Lensed GW sources. The background colored contours with color bar to the right, show the \log_{10} of the velocity induced GW phase shift, $\log_{10}(\delta\phi)$, between two strongly lensed images derived using Eq. 14, as a function of the GW frequency f , and object mass m , all defined in the observer frame. The black contour lines show the value $\delta\phi$. The overlayed pink contour lines show the corresponding GW merger time from Eq. 13. We have assumed $\theta = 25''$, and $v_d = 1000 \text{ km s}^{-1}$. As seen, for our chosen values, the GW phase shift can accumulate up to ~ 1.0 radian for next-generation ground-based detectors ($\min(f) \approx 1-5 \text{ Hz}$), whereas for LVK one expects closer to ~ 0.01 for a typical $\sim 10M_\odot + 10M_\odot$ BBH merger. Corresponding δSNR results for ET are shown in Fig. 4.

where T is the time between GW cycles (e.g. Samsing et al. 2024; Hendriks et al. 2024a,b). In this formalism, τ is the parameter that encodes information about the lensing system and the relative motion of the GW source. More information is available through the time delay and relative image magnification; however this is not directly relevant for our GW phase shift estimates considered here.

The time displacement τ , can e.g. be calculated using the time delay formalism in strong lensing systems. In a strongly lensed system, the extra time it takes for a wave packet to reach the observer along its deflected path relative to an undeflected is given by (e.g. Oguri et al. 2002),

$$\begin{aligned} \Delta t(\theta, \beta_0, \Delta\beta) &\approx \frac{D_L D_S (1+z_L)}{2c D_{LS}} \left(|(\theta - \beta_0) - \Delta\beta|^2 \right), \\ &\approx \frac{D_L D_S (1+z_L)}{2c D_{LS}} \left((\theta^2 - 2\theta\beta_0) - 2\theta\Delta\beta \right), \end{aligned} \quad (8)$$

where θ denotes the apparent angular position relative to the position of the lens, β_0 denotes the angular position of the GW source at merger, and $\beta = \beta_0 + \Delta\beta$ denotes the GW

source position at an earlier time. This relation implies that if the GW source moves from an angular position $\beta_0 + \Delta\beta$ to β_0 , then the change in time delay will be $\delta t \approx \Delta t(\theta, \beta_0, \Delta\beta) - \Delta t(\theta, \beta_0, \Delta\beta = 0)$ (see Fig. 1). This change is not directly possible to measure from a single image of a GW merger, as it will be degenerate with the velocity, redshift, or mass of the source. However, with two images the change in time delay will result in that the GW signal in one of the images will arrive earlier or later compared to the other image. This time difference is what we denote as τ , which then is $\tau \approx 2\delta t$. By now using Eq. 8 we find,

$$\tau \approx \frac{2D_L D_S (1+z_L)}{c D_{LS}} \theta \Delta\beta. \quad (9)$$

If the source is moving relative to the lens and observer then,

$$\Delta\beta = v' t'_O / D_S, \quad (10)$$

and together with relations from Eq. 5, Eq. 6, and Eq. 9, we can now write Eq. 7 as,

$$\delta\phi = 4\pi\theta f t v_d / c \quad (11)$$

where v_d is an ‘effective Doppler velocity’ given by (see e.g. Itoh et al. 2009),

$$v_d = v_O + \frac{D_L}{D_{LS}} \frac{1+z_L}{1+z_S} v_S - \frac{D_S}{D_{LS}} v_L. \quad (12)$$

Note here that the form of Eq. 11 is identical to our simple estimate given by Eq. 2, but with v given by v_d from above.

These relations provide the GW phase shift as a function of the GW frequency, f and time t in the observer frame. However, in our setup we assume the GW merger is also observed as this allows for an accurate time alignment of the GW forms received from the two images, which implies that f is related to t through the merger time. Using the relations from Peters (1964), we can express the merger time, t_m , as a function of GW frequency, f , as,

$$t_m = \frac{2^{4/3} 5}{\pi^{8/3} 512} \frac{c^5}{G^{5/3}} \times \frac{1}{m^{5/3} f^{8/3}}, \quad (13)$$

where we have assumed the case where each of the two merging compact objects have an equal mass m . By now substituting t from Eq. 11 with this expression for t_m one finds,

$$\begin{aligned} \delta\phi &= \frac{2^{4/3} 5}{\pi^{5/3} 128} \frac{c^5}{G^{5/3}} \times \frac{\theta}{m^{5/3} f^{5/3}} \frac{v_d}{c}, \\ &\approx 5 \text{ rad} \left(\frac{\theta}{25''} \right) \left(\frac{M_\odot}{m} \right)^{5/3} \left(\frac{\text{Hz}}{f} \right)^{5/3} \left(\frac{v_d / \text{km s}^{-1}}{1000} \right) \end{aligned} \quad (14)$$

where m and f are both defined in the observer frame. Fig. 2 shows the GW phase shift $\delta\phi$ (Eq. 14), and the corresponding merger time (Eq. 13), as a function of the GW frequency, f

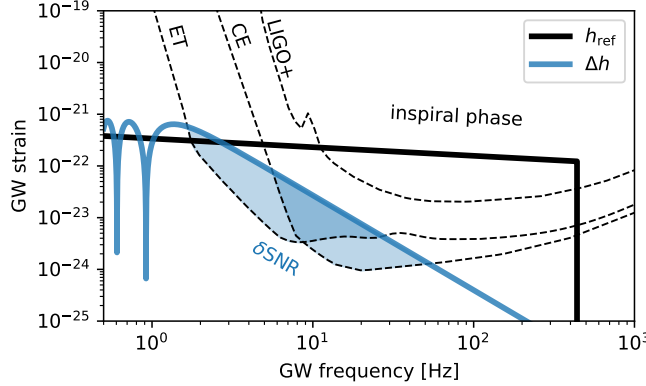


Figure 3. Strain Evolution and Detector Sensitivity. The solid black line shows two overlapping GW strains, h_1 and h_2 , that differ by a velocity induced GW phase shift, $\delta\phi$, where the solid blue line shows their difference $\Delta h = h_1 - h_2$. The specific parameters for this system is $z_L = 0.5$, $z_S = 1$, $M = 5M_\odot$, $\mu = 10$, $v_S = 3000 \text{ km s}^{-1}$, $M_L = 3 \times 10^{14} M_\odot$. The sensitivity curves for ET, CE and LIGO are shown with dashed lines. Both the planned ET and CE will operate with a sensitivity to realistically probe this effect for \sim hundreds of astrophysical lensed GW sources.

(x-axis) and BH mass m (y-axis) in the observer frame, for $\theta = 25''$ (e.g. Oguri & Blandford 2009), and $v_d = 1000 \text{ km s}^{-1}$. As seen, given the right combination of m , f and detector sensitivity range, the GW phase shift can be significant with great prospects for measurability (see also Itoh et al. 2009), as we quantify in Sec. 3 below.

3. DETECTABILITY

To estimate the detectability of the relative transverse motion over a large parameter space, we employ the δSNR criterion. The latter states that a waveform perturbation, e.g. from a Doppler shift, is detectable if the following inequality is satisfied,

$$\delta\text{SNR} \equiv \sqrt{\langle \Delta h, \Delta h \rangle} > C, \quad (15)$$

$$\Delta h = h_{\text{ref}} - h_{\text{Dopp}}, \quad (16)$$

where h_{ref} here refers to a reference waveform, and h_{Dopp} a Doppler shifted waveform. In our setup, the GW signal from one of the images is first chosen to be the reference waveform, where the GW signal from the other image will be the transverse velocity induced Doppler shifted waveform. The inner product $\langle \cdot, \cdot \rangle$ represents the noise weighted SNR h ,

$$\langle h_1, h_2 \rangle = 2 \int_0^\infty \frac{\tilde{h}_1 \tilde{h}_2^* + \tilde{h}_1^* \tilde{h}_2}{S_n(f')} df', \quad (17)$$

where \tilde{h}_i is the Fourier space representation of the waveform h_i , super script ‘*’ denotes the complex conjugate, and S_n is the noise power spectral density of a given detector. The interpretation of Eq. 15 is that the SNR of the difference

between unperturbed and perturbed waveforms must reach a certain threshold in order to be detectable. The value of C is often chosen to be 8, in analogy to the typical minimum SNR required for a confident detection in LVK. In reality, its value should depend on employed waveforms, detector properties and the specific form of the waveform perturbation. Additionally, satisfying Eq. 15 does not guarantee that a perturbation can be distinguished in the full parameter estimation procedure, due to the presence of degeneracies. Nevertheless, the δSNR criterion suffices for the purposes of this work, as it does indeed indicate whether a waveform perturbation is in principle large enough to be detectable. Furthermore, it allows to efficiently survey a large volume of phase space.

3.1. Next-Generation Ground-Based Detectors

In this work we focus on results derived for next-generation ground-based detectors, as these will see hundreds of lensed GW sources, and be highly sensitive at low GW frequencies that greatly enhances the detection of GW phase shift in general. We focus in particular on the prospects of an instrument with a noise power spectral density similar to that of ET, but our main results do generally also apply to CE. The sensitivity curves of ground-based detectors and a possible lensed GW signal are illustrated in Fig. 3, which shows the noise curves of ET, CE, and LIGO, together with a BBH strain signal, h_{ref} , and the strain difference, Δh , between this h_{ref} and a similar GW signal but Doppler shifted in phase according to Eq. 22 (see figure caption).

In the following analysis, we consider a configuration of source and lens specified by the following parameters:

$$\text{Ref. par.: } \begin{cases} z_S; & \text{Source Redshift} \\ M; & \text{Chirp mass} \\ \mu; & \text{magnification} \end{cases} \quad (18)$$

$$\text{Deph. par.: } \begin{cases} z_L; & \text{Lens Redshift} \\ M_L; & \text{Lens mass} \\ v_O; & \text{Observer velocity} \\ v_L; & \text{Lens velocity} \\ v_S; & \text{Source velocity} \end{cases} \quad (19)$$

The waveforms are generated by the analytical Newtonian result in the stationary phase approximation (Cutler & Flanagan 1994), modified with an magnification factor from the strong lensing,

$$\tilde{h}(f) = \sqrt{\mu} \frac{Q}{d(z)} \left(\frac{GM}{c^3} \right)^{5/6} f^{-7/6} \exp[i(-\phi)]. \quad (20)$$

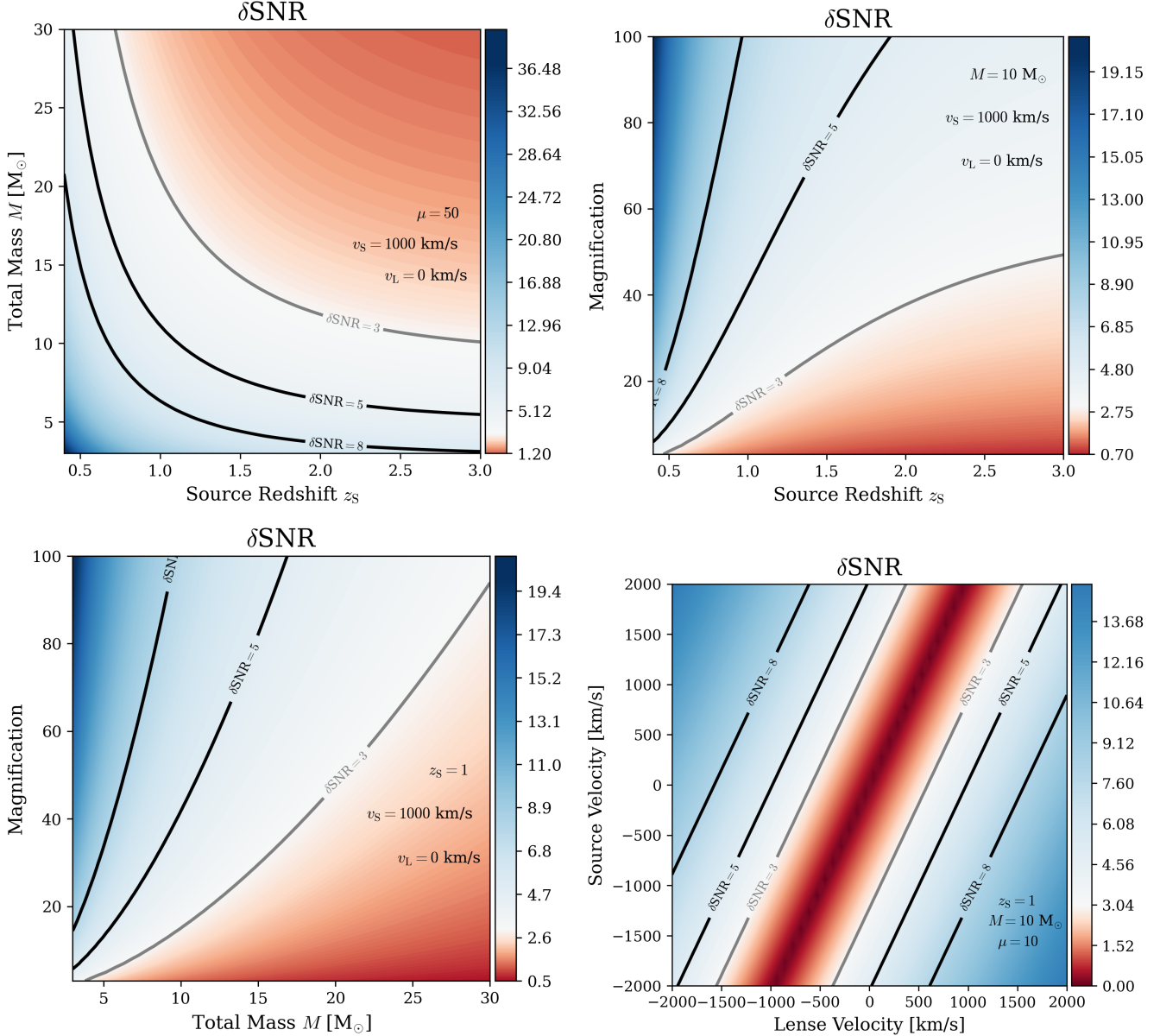


Figure 4. Einstein Telescope Detectability. The four plots each show δSNR for measuring the relative transverse velocity induced GW phase shift $\delta\phi$, between two images of a strongly lensed GW source (Sec. 3.1). This GW phase shift and its detectability depends especially on the total mass of the GW source (M), the relative velocities of the lens and source (v_L, v_S), the time evolving GW frequency (f), the source redshift (z_S), image magnification (μ), and the detector sensitivity through its noise power spectral density (see Fig. 3). The four plots show results for different combinations of these parameters. We here assume $M = 2m$, $z_L = z_S/2$ and that the magnification of each lensed image is the same.

Here f is the observed GW frequency, \mathcal{M} is the red-shifted chirp mass, $d(z)$ is the luminosity distance, Q is a geometric pre-factor that accounts for projections of the GW onto a given detector, μ is the lensing magnification factor, and ϕ is the phase

$$\phi = 2\pi f t(f) + 2(8\pi \mathcal{M} f)^{-5/3}, \quad (21)$$

where we have neglected a constant phase offset and the integration constant ϕ_c , which represents the phase at coalescence. We further assume the binary evolves with zero ec-

centricity. Following this notation, the waveform that is being considered dephased compared to the other is now given by,

$$\phi_{\text{Dopp}} = \phi_{\text{ref}} + \delta\phi(M_L, z_L, z_S, v_L, v_S, v_O). \quad (22)$$

where $\delta\phi$ is the GW phase shift described by Eq. 14. The δSNR is then estimated from Δh , that is calculated using Eq. 20 with ϕ_{ref} and ϕ_{Dopp} as input.

Results for ET are shown in Fig. 4, which shows contours of δSNR as a function of the relevant parameters in our setup. We here assume that both GW signals have the same mag-

nification, the lens redshift relates to the source redshift as $z_L = z_S/2$, and that the lens mass is $M_L = 3 \times 10^{14} M_\odot$. Regarding our chosen values of parameters in the plots, we point out that current models and observations by LIGO hint that the single BH mass spectrum peaks around $5 \sim 10 M_\odot$ (e.g. Abbott et al. 2019a), the source redshift z_s peaks for strong lensing ~ 2 for ET (e.g. Xu et al. 2022), galaxy clusters have a typical velocity dispersion $\mathcal{O}(1000 \text{ km s}^{-1})$, and the lensing kernel in lens mass peaks around $10^{14} M_\odot$, with larger lens masses preferred for low redshift sources (e.g. Xu et al. 2022; Smith et al. 2023). In addition, the lensing magnification can span 2-3 orders of magnitude (e.g. Savastano et al. 2024).

We first consider the *upper left plot* which shows δSNR , as a function of z_S and total rest frame GW source mass M , for $v_S = 1000 \text{ km s}^{-1}$, $v_L = 0 \text{ km s}^{-1}$, and $\mu = 50$. For these values, a robust detection for $z_S \lesssim 1$ of transverse velocity with $\delta\text{SNR} \sim 8$ is possible for GW sources with total mass up to $\sim 5 M_\odot - 10 M_\odot$ with a steep dependence on z_S . If one allows for a slightly lower δSNR threshold, the available space significantly opens up, implying that GW sources up to $z_S \sim 1$ with a total mass up in the range of $\sim 10 M_\odot - 30 M_\odot$ will show detectable features arising from transverse velocities. The *upper right plot* shows δSNR , as a function of z_S and magnification μ , for a fixed total GW source mass of $M = 10 M_\odot$. As seen, for a δSNR of ~ 5 , a magnification of $\mu \sim 40$ is required for claiming detection at $z_S \sim 1$, where $\mu \sim 100$ will bring the horizon out to $z_S \sim 2.0$. The *lower left plot* shows instead the dependence on mass M for fixed $z_S = 1$. This especially shows that the μ has to be greater than ~ 40 for systems with $M \sim 10 M_\odot$ for our chosen relative velocity to be resolved. The *lower right plot* shows the dependence on v_L and v_S , which enter into the GW phase shift with different weight factors set by the geometry and cosmology as seen in Eq. 12. This is clearly seen in the δSNR contours, e.g. for $v_L = 0 \text{ km s}^{-1}$ and $v_S \pm 1000 \text{ km s}^{-1}$ the maximum δSNR is < 3 , whereas for $v_S = 0 \text{ km s}^{-1}$ and $v_L \pm 1000 \text{ km s}^{-1}$ the maximum δSNR is > 5 . The two velocities can naturally also add up constructively, resulting for our chosen setup in a $\delta\text{SNR} \sim 8$ if the source and the lens move opposite to each other with a velocity of $\sim 1000 \text{ km s}^{-1}$ each, which is certainly not unreasonably.

To conclude, our considered examples definitely hint that it should be possible to put constraints on the relative transverse velocity of GW sources that falls into the regime of real astrophysical systems. We have only considered a small part of the relevant phase space here, but our results serve as a major motivation to study this in greater detail.

4. CONCLUSIONS

We have in this paper illustrated the possibility of measuring the relative transverse motion of GW sources in strong lens systems, when two or more images of the GW source is

observed (see Fig. 1). This is possible as the strong lensed images essentially allow the observer to see the GW source from different lines-of-sight, each of which will show different projections of the relative velocity of the GW source. This gives rise to a differential Doppler shift between the images, which can be translated to an observable GW phase shift (see also Itoh et al. 2009).

If more than two images are observed, one can triangulate using image pairs, or a joint fit, for the transverse velocity vector in the source plane; we therefore refer to this technique as *Doppler-Triangulation*. This method provides opportunities of getting a rare glimpse into how GW sources move relative to the cosmic flow, which otherwise is impossible to measure using single GW signals alone. We have focused on cosmological lensed configurations, as we know that strongly lensed GW sources will be observed in the near future (Xu et al. 2022; Smith et al. 2023), but the effect we are describing could happen for any other system where lens and source move relative to each other (see also Yang et al. 2024; Savastano et al. 2024).

Using a δSNR criterion we quantified the observable possibilities for ET, as this is expected to detect hundreds of lensed GW systems (e.g. Xu et al. 2022; Smith et al. 2023). For reasonable parameters of total BBH mass $M \sim \mathcal{O}(10 M_\odot)$, relative velocity $v \sim \mathcal{O}(1000 \text{ km s}^{-1})$, lensing magnification $\mu \sim \mathcal{O}(10)$, source redshift $z_S \sim \mathcal{O}(1)$, and lens mass $\mathcal{O}(10^{14} M_\odot)$, we find that measuring the resultant GW phase shift between pairwise images should definitely be possible. This opens up tremendous opportunities for ET as well as CE to probe the relative transverse flow of GW sources, which undoubtedly will give better hints to where and how these systems are forming in our Universe.

It is natural to follow up on our study with a more detailed analysis using a realistic lens model, lens and source distributions, as well as including more than two images to quantify how well one can triangulate for the full relative transverse velocity vector. It is also of high interest to quantify, possibly using state-of-the-art cosmological simulations, if different GW source populations are expected to have statistically different velocity distributions as a function of redshift. Using simulations and observational constraints, combined with GW source population codes, we plan on looking into this in upcoming papers.

5. ACKNOWLEDGMENTS

The authors are grateful Juan Urrutia, Mikołaj Korzyński, Miguel Zumalacárregui, and Graham Smith, for useful discussions. We further thank the The Erwin Schrödinger International Institute for Mathematics and Physics (ESI) and the organizers of the workshop "Lensing and Wave Optics in Strong Gravity" where part of this work was carried out. K.H, L.Z., P.S., and J.S. are supported by the Villum Fonden grant

No. 29466, and by the ERC Starting Grant no. 101043143 – BlackHoleMergs led by J. Samsing. J.M.E, R.L and L.V. are supported by the research grant no. VIL37766 and no. VIL53101 from Villum Fonden, and the DNRF Chair program grant no. DNRF162 by the Danish National Re-

search Foundation. J.M.E. is also supported by the Marie Skłodowska-Curie grant agreement No. 847523 INTERACTIONS. The Tycho supercomputer hosted at the SCIENCE HPC center at the University of Copenhagen was used for supporting this work.

REFERENCES

- Abbott, B. P., Abbott, R., Abbott, T. D., et al. 2019a, ApJL, 882, L24, doi: [10.3847/2041-8213/ab3800](https://doi.org/10.3847/2041-8213/ab3800)
- . 2019b, ApJ, 883, 149, doi: [10.3847/1538-4357/ab3c2d](https://doi.org/10.3847/1538-4357/ab3c2d)
- Abbott, R., Abbott, T. D., Abraham, S., et al. 2020, PhRvL, 125, 101102, doi: [10.1103/PhysRevLett.125.101102](https://doi.org/10.1103/PhysRevLett.125.101102)
- Abbott, R., et al. 2021, Astrophys. J., 923, 14, doi: [10.3847/1538-4357/ac23db](https://doi.org/10.3847/1538-4357/ac23db)
- Abbott, R., Abe, H., Acernese, F., et al. 2023, ApJS, 267, 29, doi: [10.3847/1538-4365/acdc9f](https://doi.org/10.3847/1538-4365/acdc9f)
- Abbott, R., et al. 2024, Astrophys. J., 970, 191, doi: [10.3847/1538-4357/ad3e83](https://doi.org/10.3847/1538-4357/ad3e83)
- Antognini, J. M. O., & Thompson, T. A. 2016, MNRAS, 456, 4219, doi: [10.1093/mnras/stv2938](https://doi.org/10.1093/mnras/stv2938)
- Antonini, F., Chatterjee, S., Rodriguez, C. L., et al. 2016, ApJ, 816, 65, doi: [10.3847/0004-637X/816/2/65](https://doi.org/10.3847/0004-637X/816/2/65)
- Antonini, F., & Rasio, F. A. 2016, ApJ, 831, 187, doi: [10.3847/0004-637X/831/2/187](https://doi.org/10.3847/0004-637X/831/2/187)
- Askar, A., Szkudlarek, M., Gondek-Rosińska, D., Giersz, M., & Bulik, T. 2017, MNRAS, 464, L36, doi: [10.1093/mnrasl/slw177](https://doi.org/10.1093/mnrasl/slw177)
- Atallah, D., Trani, A. A., Kremer, K., et al. 2023, MNRAS, 523, 4227, doi: [10.1093/mnras/stad1634](https://doi.org/10.1093/mnras/stad1634)
- Bae, Y.-B., Kim, C., & Lee, H. M. 2014, MNRAS, 440, 2714, doi: [10.1093/mnras/stu381](https://doi.org/10.1093/mnras/stu381)
- Banerjee, S., Baumgardt, H., & Kroupa, P. 2010, MNRAS, 402, 371, doi: [10.1111/j.1365-2966.2009.15880.x](https://doi.org/10.1111/j.1365-2966.2009.15880.x)
- Barausse, E., Cardoso, V., & Pani, P. 2014, PhRvD, 89, 104059, doi: [10.1103/PhysRevD.89.104059](https://doi.org/10.1103/PhysRevD.89.104059)
- Bartos, I., Kocsis, B., Haiman, Z., & Márka, S. 2017, ApJ, 835, 165, doi: [10.3847/1538-4357/835/2/165](https://doi.org/10.3847/1538-4357/835/2/165)
- Beheshti, A., Schaan, E., & Kosowsky, A. 2024, arXiv e-prints, arXiv:2408.16055, doi: [10.48550/arXiv.2408.16055](https://doi.org/10.48550/arXiv.2408.16055)
- Belczynski, K., Holz, D. E., Bulik, T., & O’Shaughnessy, R. 2016a, Nature, 534, 512, doi: [10.1038/nature18322](https://doi.org/10.1038/nature18322)
- Belczynski, K., Repetto, S., Holz, D. E., et al. 2016b, ApJ, 819, 108, doi: [10.3847/0004-637X/819/2/108](https://doi.org/10.3847/0004-637X/819/2/108)
- Bird, S., Cholis, I., Muñoz, J. B., et al. 2016, Physical Review Letters, 116, 201301, doi: [10.1103/PhysRevLett.116.201301](https://doi.org/10.1103/PhysRevLett.116.201301)
- Birkinshaw, M. 1989, in Gravitational Lenses, ed. J. M. Moran, J. N. Hewitt, & K.-Y. Lo, Vol. 330, 59, doi: [10.1007/3-540-51061-3_36](https://doi.org/10.1007/3-540-51061-3_36)
- Biscoveanu, S., Callister, T. A., Haster, C.-J., et al. 2022, ApJL, 932, L19, doi: [10.3847/2041-8213/ac71a8](https://doi.org/10.3847/2041-8213/ac71a8)
- Breivik, K., Rodriguez, C. L., Larson, S. L., Kalogera, V., & Rasio, F. A. 2016, ApJL, 830, L18, doi: [10.3847/2041-8205/830/1/L18](https://doi.org/10.3847/2041-8205/830/1/L18)
- Carr, B., Kühnel, F., & Sandstad, M. 2016, PhRvD, 94, 083504, doi: [10.1103/PhysRevD.94.083504](https://doi.org/10.1103/PhysRevD.94.083504)
- Çalışkan, M., Anil Kumar, N., Ji, L., et al. 2023, Phys. Rev. D, 108, 123543, doi: [10.1103/PhysRevD.108.123543](https://doi.org/10.1103/PhysRevD.108.123543)
- Chamberlain, K., Moore, C. J., Gerosa, D., & Yunes, N. 2019, PhRvD, 99, 024025, doi: [10.1103/PhysRevD.99.024025](https://doi.org/10.1103/PhysRevD.99.024025)
- Chen, A., Cremonese, P., Ezquiaga, J. M., & Keitel, D. 2024, Phys. Rev. D, 110, 123015, doi: [10.1103/PhysRevD.110.123015](https://doi.org/10.1103/PhysRevD.110.123015)
- Chen, X., & Amaro-Seoane, P. 2017, ApJL, 842, L2, doi: [10.3847/2041-8213/aa74ce](https://doi.org/10.3847/2041-8213/aa74ce)
- Chitre, S. M., & Saslaw, W. C. 1989, Nature, 341, 38, doi: [10.1038/341038a0](https://doi.org/10.1038/341038a0)
- Cholis, I., Kovetz, E. D., Ali-Haïmoud, Y., et al. 2016, PhRvD, 94, 084013, doi: [10.1103/PhysRevD.94.084013](https://doi.org/10.1103/PhysRevD.94.084013)
- Cremonese, P., Ezquiaga, J. M., & Salzano, V. 2021, Phys. Rev. D, 104, 023503, doi: [10.1103/PhysRevD.104.023503](https://doi.org/10.1103/PhysRevD.104.023503)
- Cutler, C., & Flanagan, É. E. 1994, PhRvD, 49, 2658, doi: [10.1103/PhysRevD.49.2658](https://doi.org/10.1103/PhysRevD.49.2658)
- Dai, L., Zackay, B., Venumadhav, T., Roulet, J., & Zaldarriaga, M. 2020, arXiv e-prints, arXiv:2007.12709, doi: [10.48550/arXiv.2007.12709](https://doi.org/10.48550/arXiv.2007.12709)
- Dominik, M., Belczynski, K., Fryer, C., et al. 2012, ApJ, 759, 52, doi: [10.1088/0004-637X/759/1/52](https://doi.org/10.1088/0004-637X/759/1/52)
- . 2013, ApJ, 779, 72, doi: [10.1088/0004-637X/779/1/72](https://doi.org/10.1088/0004-637X/779/1/72)
- Dominik, M., Berti, E., O’Shaughnessy, R., et al. 2015, ApJ, 806, 263, doi: [10.1088/0004-637X/806/2/263](https://doi.org/10.1088/0004-637X/806/2/263)
- D’Orazio, D. J., & Loeb, A. 2018, PhRvD, 97, 083008, doi: [10.1103/PhysRevD.97.083008](https://doi.org/10.1103/PhysRevD.97.083008)
- . 2020, PhRvD, 101, 083031, doi: [10.1103/PhysRevD.101.083031](https://doi.org/10.1103/PhysRevD.101.083031)
- D’Orazio, D. J., & Samsing, J. 2018, MNRAS, 481, 4775, doi: [10.1093/mnras/sty2568](https://doi.org/10.1093/mnras/sty2568)
- Ezquiaga, J. M., & Holz, D. E. 2022, Phys. Rev. Lett., 129, 061102, doi: [10.1103/PhysRevLett.129.061102](https://doi.org/10.1103/PhysRevLett.129.061102)
- Ezquiaga, J. M., Holz, D. E., Hu, W., Lagos, M., & Wald, R. M. 2021, Phys. Rev. D, 103, 064047, doi: [10.1103/PhysRevD.103.064047](https://doi.org/10.1103/PhysRevD.103.064047)
- Ezquiaga, J. M., & Zumalacárregui, M. 2020, Phys. Rev. D, 102, 124048, doi: [10.1103/PhysRevD.102.124048](https://doi.org/10.1103/PhysRevD.102.124048)

- Fabj, G., & Samsing, J. 2024, arXiv e-prints, arXiv:2402.16948.
<https://arxiv.org/pdf/2402.16948.pdf>
- Farr, W. M., Fishbach, M., Ye, J., & Holz, D. E. 2019, ApJL, 883, L42, doi: [10.3847/2041-8213/ab4284](https://doi.org/10.3847/2041-8213/ab4284)
- Fishbach, M., & Fragione, G. 2023, MNRAS, 522, 5546, doi: [10.1093/mnras/stad1364](https://doi.org/10.1093/mnras/stad1364)
- Fishbach, M., Holz, D. E., & Farr, W. M. 2018, ApJL, 863, L41, doi: [10.3847/2041-8213/aad800](https://doi.org/10.3847/2041-8213/aad800)
- García-Bellido, J., Nuño Siles, J. F., & Ruiz Morales, E. 2021, Physics of the Dark Universe, 31, 100791, doi: [10.1016/j.dark.2021.100791](https://doi.org/10.1016/j.dark.2021.100791)
- Garg, M., Derdzinski, A., Zwick, L., Capelo, P. R., & Mayer, L. 2022, MNRAS, 517, 1339, doi: [10.1093/mnras/stac2711](https://doi.org/10.1093/mnras/stac2711)
- Gayathri, V., Healy, J., Lange, J., et al. 2022, Nature Astronomy, 6, 344, doi: [10.1038/s41550-021-01568-w](https://doi.org/10.1038/s41550-021-01568-w)
- Gondán, L., & Kocsis, B. 2022, MNRAS, 515, 3299, doi: [10.1093/mnras/stac1985](https://doi.org/10.1093/mnras/stac1985)
- Goyal, S., Haris, K., Mehta, A. K., & Ajith, P. 2021, Phys. Rev. D, 103, 024038, doi: [10.1103/PhysRevD.103.024038](https://doi.org/10.1103/PhysRevD.103.024038)
- Goyal, S., Vijaykumar, A., Ezquiaga, J. M., & Zumalacarregui, M. 2023, Phys. Rev. D, 108, 024052, doi: [10.1103/PhysRevD.108.024052](https://doi.org/10.1103/PhysRevD.108.024052)
- Gültekin, K., Miller, M. C., & Hamilton, D. P. 2006, ApJ, 640, 156
- Gupte, N., Ramos-Buades, A., Buonanno, A., et al. 2024, arXiv e-prints, arXiv:2404.14286, doi: [10.48550/arXiv.2404.14286](https://doi.org/10.48550/arXiv.2404.14286)
- Hamers, A. S., Bar-Or, B., Petrovich, C., & Antonini, F. 2018, ApJ, 865, 2, doi: [10.3847/1538-4357/aadae2](https://doi.org/10.3847/1538-4357/aadae2)
- Hamers, A. S., & Thompson, T. A. 2019, ApJ, 883, 23, doi: [10.3847/1538-4357/ab3b06](https://doi.org/10.3847/1538-4357/ab3b06)
- Hendriks, K., Zwick, L., & Samsing, J. 2024a, arXiv e-prints, arXiv:2408.04603, doi: [10.48550/arXiv.2408.04603](https://doi.org/10.48550/arXiv.2408.04603)
- Hendriks, K., Atallah, D., Martinez, M., et al. 2024b, arXiv e-prints, arXiv:2411.08572, doi: [10.48550/arXiv.2411.08572](https://doi.org/10.48550/arXiv.2411.08572)
- Hoang, B.-M., Naoz, S., Kocsis, B., Rasio, F. A., & Dosopoulou, F. 2018, ApJ, 856, 140, doi: [10.3847/1538-4357/aaafce](https://doi.org/10.3847/1538-4357/aaafce)
- Hong, J., & Lee, H. M. 2015, MNRAS, 448, 754, doi: [10.1093/mnras/stv035](https://doi.org/10.1093/mnras/stv035)
- Hotinli, S. C., Smith, K. M., Madhavacheril, M. S., & Kamionkowski, M. 2021, PhRvD, 104, 083529, doi: [10.1103/PhysRevD.104.083529](https://doi.org/10.1103/PhysRevD.104.083529)
- Hu, W.-R., & Wu, Y.-L. 2017, National Science Review, 4, 685, doi: [10.1093/nsr/nwx116](https://doi.org/10.1093/nsr/nwx116)
- Inayoshi, K., Tamanini, N., Caprini, C., & Haiman, Z. 2017, PhRvD, 96, 063014, doi: [10.1103/PhysRevD.96.063014](https://doi.org/10.1103/PhysRevD.96.063014)
- Iorio, G., Mapelli, M., Costa, G., et al. 2023, MNRAS, 524, 426, doi: [10.1093/mnras/stad1630](https://doi.org/10.1093/mnras/stad1630)
- Itoh, Y., Futamase, T., & Hattori, M. 2009, PhRvD, 80, 044009, doi: [10.1103/PhysRevD.80.044009](https://doi.org/10.1103/PhysRevD.80.044009)
- Jana, S., Kapadia, S. J., Venumadhav, T., & Ajith, P. 2023, Phys. Rev. Lett., 130, 261401, doi: [10.1103/PhysRevLett.130.261401](https://doi.org/10.1103/PhysRevLett.130.261401)
- Janiuk, A., Bejger, M., Charzyński, S., & Sukova, P. 2017, ArXiv e-prints, 51, 7, doi: [10.1016/j.newast.2016.08.002](https://doi.org/10.1016/j.newast.2016.08.002)
- Kalogera, V. 2000, ApJ, 541, 319, doi: [10.1086/309400](https://doi.org/10.1086/309400)
- Kawamura, S., Ando, M., Seto, N., et al. 2011, Classical and Quantum Gravity, 28, 094011, doi: [10.1088/0264-9381/28/9/094011](https://doi.org/10.1088/0264-9381/28/9/094011)
- Kayser, R., Refsdal, S., & Stabell, R. 1986, A&A, 166, 36
- Kremer, K., Rodriguez, C. L., Amaro-Seoane, P., et al. 2019, PhRvD, 99, 063003, doi: [10.1103/PhysRevD.99.063003](https://doi.org/10.1103/PhysRevD.99.063003)
- Laeuger, A., Seymour, B., Chen, Y., & Yu, H. 2023, arXiv e-prints, arXiv:2310.16799, doi: [10.48550/arXiv.2310.16799](https://doi.org/10.48550/arXiv.2310.16799)
- Lee, W. H., Ramirez-Ruiz, E., & van de Ven, G. 2010, ApJ, 720, 953
- Li, G., Naoz, S., Kocsis, B., & Loeb, A. 2014, ApJ, 785, 116, doi: [10.1088/0004-637X/785/2/116](https://doi.org/10.1088/0004-637X/785/2/116)
- Liu, B., & Lai, D. 2018, ApJ, 863, 68, doi: [10.3847/1538-4357/aad09f](https://doi.org/10.3847/1538-4357/aad09f)
- . 2021, MNRAS, 502, 2049, doi: [10.1093/mnras/stab178](https://doi.org/10.1093/mnras/stab178)
- Liu, B., Lai, D., & Wang, Y.-H. 2019a, ApJL, 883, L7, doi: [10.3847/2041-8213/ab40c0](https://doi.org/10.3847/2041-8213/ab40c0)
- . 2019b, ApJ, 881, 41, doi: [10.3847/1538-4357/ab2dfb](https://doi.org/10.3847/1538-4357/ab2dfb)
- Liu, S., Hu, Y.-M., Zhang, J.-d., & Mei, J. 2020, PhRvD, 101, 103027, doi: [10.1103/PhysRevD.101.103027](https://doi.org/10.1103/PhysRevD.101.103027)
- Loeb, A. 2016, ApJL, 819, L21, doi: [10.3847/2041-8205/819/2/L21](https://doi.org/10.3847/2041-8205/819/2/L21)
- Luo, J., Chen, L.-S., Duan, H.-Z., et al. 2016, Classical and Quantum Gravity, 33, 035010, doi: [10.1088/0264-9381/33/3/035010](https://doi.org/10.1088/0264-9381/33/3/035010)
- Martinez, M. A. S., Fragione, G., Kremer, K., et al. 2020, ApJ, 903, 67, doi: [10.3847/1538-4357/abba25](https://doi.org/10.3847/1538-4357/abba25)
- McKernan, B., Ford, K. E. S., Bellovary, J., et al. 2017, ArXiv e-prints. <https://arxiv.org/abs/1702.07818>
- Meiron, Y., Kocsis, B., & Loeb, A. 2017, ApJ, 834, 200, doi: [10.3847/1538-4357/834/2/200](https://doi.org/10.3847/1538-4357/834/2/200)
- Murguia-Berthier, A., MacLeod, M., Ramirez-Ruiz, E., Antoni, A., & Macias, P. 2017, ApJ, 845, 173, doi: [10.3847/1538-4357/aa8140](https://doi.org/10.3847/1538-4357/aa8140)
- Naoz, S., Kocsis, B., Loeb, A., & Yunes, N. 2013, ApJ, 773, 187, doi: [10.1088/0004-637X/773/2/187](https://doi.org/10.1088/0004-637X/773/2/187)
- Oguri, M., & Blandford, R. D. 2009, MNRAS, 392, 930, doi: [10.1111/j.1365-2966.2008.14154.x](https://doi.org/10.1111/j.1365-2966.2008.14154.x)
- Oguri, M., Taruya, A., Suto, Y., & Turner, E. L. 2002, ApJ, 568, 488, doi: [10.1086/339064](https://doi.org/10.1086/339064)
- O’Leary, R. M., Kocsis, B., & Loeb, A. 2009, MNRAS, 395, 2127, doi: [10.1111/j.1365-2966.2009.14653.x](https://doi.org/10.1111/j.1365-2966.2009.14653.x)
- Park, D., Kim, C., Lee, H. M., Bae, Y.-B., & Belczynski, K. 2017, MNRAS, 469, 4665, doi: [10.1093/mnras/stx1015](https://doi.org/10.1093/mnras/stx1015)
- Peters, P. C. 1964, Physical Review, 136, 1224, doi: [10.1103/PhysRev.136.B1224](https://doi.org/10.1103/PhysRev.136.B1224)

- Pijnenburg, M., Cusin, G., Pitrou, C., & Uzan, J.-P. 2024, PhRvD, 110, 044054, doi: [10.1103/PhysRevD.110.044054](https://doi.org/10.1103/PhysRevD.110.044054)
- Portegies Zwart, S. F., & McMillan, S. L. W. 2000, ApJ, 528, L17
- Ramirez-Ruiz, E., Trenti, M., MacLeod, M., et al. 2015, ApJL, 802, L22, doi: [10.1088/2041-8205/802/2/L22](https://doi.org/10.1088/2041-8205/802/2/L22)
- Randall, L., & Xianyu, Z.-Z. 2018, ApJ, 864, 134, doi: [10.3847/1538-4357/aad7fe](https://doi.org/10.3847/1538-4357/aad7fe)
- . 2019, ApJ, 878, 75, doi: [10.3847/1538-4357/ab20c6](https://doi.org/10.3847/1538-4357/ab20c6)
- Robson, T., Cornish, N. J., Tamanini, N., & Toonen, S. 2018, PhRvD, 98, 064012, doi: [10.1103/PhysRevD.98.064012](https://doi.org/10.1103/PhysRevD.98.064012)
- Rodriguez, C. L., Amaro-Seoane, P., Chatterjee, S., et al. 2018, PhRvD, 98, 123005, doi: [10.1103/PhysRevD.98.123005](https://doi.org/10.1103/PhysRevD.98.123005)
- Rodriguez, C. L., & Antonini, F. 2018, ApJ, 863, 7, doi: [10.3847/1538-4357/aacea4](https://doi.org/10.3847/1538-4357/aacea4)
- Rodriguez, C. L., Chatterjee, S., & Rasio, F. A. 2016a, PhRvD, 93, 084029, doi: [10.1103/PhysRevD.93.084029](https://doi.org/10.1103/PhysRevD.93.084029)
- Rodriguez, C. L., Haster, C.-J., Chatterjee, S., Kalogera, V., & Rasio, F. A. 2016b, ApJL, 824, L8, doi: [10.3847/2041-8205/824/1/L8](https://doi.org/10.3847/2041-8205/824/1/L8)
- Rodriguez, C. L., Morscher, M., Pattabiraman, B., et al. 2015, PhRvL, 115, 051101, doi: [10.1103/PhysRevLett.115.051101](https://doi.org/10.1103/PhysRevLett.115.051101)
- Rodriguez, C. L., Zevin, M., Pankow, C., Kalogera, V., & Rasio, F. A. 2016c, ApJL, 832, L2, doi: [10.3847/2041-8205/832/1/L2](https://doi.org/10.3847/2041-8205/832/1/L2)
- Rom, B., Sari, R., & Lai, D. 2024, ApJ, 964, 43, doi: [10.3847/1538-4357/ad284b](https://doi.org/10.3847/1538-4357/ad284b)
- Romero-Shaw, I., Lasky, P. D., & Thrane, E. 2021a, ApJL, 921, L31, doi: [10.3847/2041-8213/ac3138](https://doi.org/10.3847/2041-8213/ac3138)
- . 2022, ApJ, 940, 171, doi: [10.3847/1538-4357/ac9798](https://doi.org/10.3847/1538-4357/ac9798)
- Romero-Shaw, I. M., Kremer, K., Lasky, P. D., Thrane, E., & Samsing, J. 2021b, MNRAS, 506, 2362, doi: [10.1093/mnras/stab1815](https://doi.org/10.1093/mnras/stab1815)
- Samsing, J. 2018, PhRvD, 97, 103014, doi: [10.1103/PhysRevD.97.103014](https://doi.org/10.1103/PhysRevD.97.103014)
- Samsing, J., Askar, A., & Giersz, M. 2018a, ApJ, 855, 124, doi: [10.3847/1538-4357/aaab52](https://doi.org/10.3847/1538-4357/aaab52)
- Samsing, J., & D’Orazio, D. J. 2018, MNRAS, doi: [10.1093/mnras/sty2334](https://doi.org/10.1093/mnras/sty2334)
- Samsing, J., D’Orazio, D. J., Kremer, K., Rodriguez, C. L., & Askar, A. 2020, PhRvD, 101, 123010, doi: [10.1103/PhysRevD.101.123010](https://doi.org/10.1103/PhysRevD.101.123010)
- Samsing, J., Hamers, A. S., & Tyles, J. G. 2019, PhRvD, 100, 043010, doi: [10.1103/PhysRevD.100.043010](https://doi.org/10.1103/PhysRevD.100.043010)
- Samsing, J., Hendriks, K., Zwick, L., D’Orazio, D. J., & Liu, B. 2024, arXiv e-prints, arXiv:2403.05625, doi: [10.48550/arXiv.2403.05625](https://doi.org/10.48550/arXiv.2403.05625)
- Samsing, J., & Ilan, T. 2018, MNRAS, 476, 1548, doi: [10.1093/mnras/sty197](https://doi.org/10.1093/mnras/sty197)
- Samsing, J., MacLeod, M., & Ramirez-Ruiz, E. 2014, ApJ, 784, 71, doi: [10.1088/0004-637X/784/1/71](https://doi.org/10.1088/0004-637X/784/1/71)
- . 2018b, ApJ, 853, 140, doi: [10.3847/1538-4357/aaa715](https://doi.org/10.3847/1538-4357/aaa715)
- Samsing, J., & Ramirez-Ruiz, E. 2017, ApJL, 840, L14, doi: [10.3847/2041-8213/aa6f0b](https://doi.org/10.3847/2041-8213/aa6f0b)
- Samsing, J., Bartos, I., D’Orazio, D. J., et al. 2022, Nature, 603, 237, doi: [10.1038/s41586-021-04333-1](https://doi.org/10.1038/s41586-021-04333-1)
- Sasaki, M., Suyama, T., Tanaka, T., & Yokoyama, S. 2016, Physical Review Letters, 117, 061101, doi: [10.1103/PhysRevLett.117.061101](https://doi.org/10.1103/PhysRevLett.117.061101)
- Savastano, S., Vernizzi, F., & Zumalacárregui, M. 2024, PhRvD, 109, 024064, doi: [10.1103/PhysRevD.109.024064](https://doi.org/10.1103/PhysRevD.109.024064)
- Schröder, S. L., Batta, A., & Ramirez-Ruiz, E. 2018, ApJL, 862, L3, doi: [10.3847/2041-8213/aacf8d](https://doi.org/10.3847/2041-8213/aacf8d)
- Silsbee, K., & Tremaine, S. 2017, ApJ, 836, 39, doi: [10.3847/1538-4357/aa5729](https://doi.org/10.3847/1538-4357/aa5729)
- Smith, G. P., Robertson, A., Mahler, G., et al. 2023, MNRAS, 520, 702, doi: [10.1093/mnras/stad140](https://doi.org/10.1093/mnras/stad140)
- Stephan, A. P., Naoz, S., Ghez, A. M., et al. 2016, MNRAS, 460, 3494, doi: [10.1093/mnras/stw1220](https://doi.org/10.1093/mnras/stw1220)
- Stone, N. C., Metzger, B. D., & Haiman, Z. 2017, MNRAS, 464, 946, doi: [10.1093/mnras/stw2260](https://doi.org/10.1093/mnras/stw2260)
- Strokov, V., Fragione, G., Wong, K. W. K., Helper, T., & Berti, E. 2022, PhRvD, 105, 124048, doi: [10.1103/PhysRevD.105.124048](https://doi.org/10.1103/PhysRevD.105.124048)
- Tagawa, H., Haiman, Z., & Kocsis, B. 2020, ApJ, 898, 25, doi: [10.3847/1538-4357/ab9b8c](https://doi.org/10.3847/1538-4357/ab9b8c)
- Takahashi, R., & Nakamura, T. 2003, ApJ, 595, 1039, doi: [10.1086/377430](https://doi.org/10.1086/377430)
- Tamanini, N., Klein, A., Bonvin, C., Barausse, E., & Caprini, C. 2020, PhRvD, 101, 063002, doi: [10.1103/PhysRevD.101.063002](https://doi.org/10.1103/PhysRevD.101.063002)
- Tambalo, G., Zumalacárregui, M., Dai, L., & Cheung, M. H.-Y. 2023, Phys. Rev. D, 108, 103529, doi: [10.1103/PhysRevD.108.103529](https://doi.org/10.1103/PhysRevD.108.103529)
- Tambalo, G., Zumalacárregui, M., Dai, L., & Cheung, M. H.-Y. 2023, PhRvD, 108, 043527, doi: [10.1103/PhysRevD.108.043527](https://doi.org/10.1103/PhysRevD.108.043527)
- Tanikawa, A. 2013, MNRAS, 435, 1358, doi: [10.1093/mnras/stt1380](https://doi.org/10.1093/mnras/stt1380)
- The LIGO Scientific Collaboration, the Virgo Collaboration, the KAGRA Collaboration, et al. 2023, arXiv e-prints, arXiv:2308.03822, doi: [10.48550/arXiv.2308.03822](https://doi.org/10.48550/arXiv.2308.03822)
- Tiwari, A., Vijaykumar, A., Kapadia, S. J., Fragione, G., & Chatterjee, S. 2024, MNRAS, 527, 8586, doi: [10.1093/mnras/stad3749](https://doi.org/10.1093/mnras/stad3749)
- Toubiana, A., Sberna, L., Caputo, A., et al. 2021, PhRvL, 126, 101105, doi: [10.1103/PhysRevLett.126.101105](https://doi.org/10.1103/PhysRevLett.126.101105)
- Trani, A. A., Quaini, S., & Colpi, M. 2023, arXiv e-prints, arXiv:2312.13281, doi: [10.48550/arXiv.2312.13281](https://doi.org/10.48550/arXiv.2312.13281)
- Trani, A. A., Rastello, S., Di Carlo, U. N., et al. 2022, MNRAS, 511, 1362, doi: [10.1093/mnras/stac122](https://doi.org/10.1093/mnras/stac122)
- Trani, A. A., Spera, M., Leigh, N. W. C., & Fujii, M. S. 2019, ApJ, 885, 135, doi: [10.3847/1538-4357/ab480a](https://doi.org/10.3847/1538-4357/ab480a)

- Trani, A. A., Tanikawa, A., Fujii, M. S., Leigh, N. W. C., & Kumamoto, J. 2021, MNRAS, 504, 910, doi: [10.1093/mnras/stab967](https://doi.org/10.1093/mnras/stab967)
- van Son, L. A. C., de Mink, S. E., Callister, T., et al. 2022, ApJ, 931, 17, doi: [10.3847/1538-4357/ac64a3](https://doi.org/10.3847/1538-4357/ac64a3)
- VanLandingham, J. H., Miller, M. C., Hamilton, D. P., & Richardson, D. C. 2016, ApJ, 828, 77, doi: [10.3847/0004-637X/828/2/77](https://doi.org/10.3847/0004-637X/828/2/77)
- Vijaykumar, A., Tiwari, A., Kapadia, S. J., Arun, K. G., & Ajith, P. 2023, ApJ, 954, 105, doi: [10.3847/1538-4357/acd77d](https://doi.org/10.3847/1538-4357/acd77d)
- Wong, K. W. K., Baibhav, V., & Berti, E. 2019, MNRAS, 488, 5665, doi: [10.1093/mnras/stz2077](https://doi.org/10.1093/mnras/stz2077)
- Woosley, S. E. 2016, ApJL, 824, L10, doi: [10.3847/2041-8205/824/1/L10](https://doi.org/10.3847/2041-8205/824/1/L10)
- Wucknitz, O., & Sperhake, U. 2004, PhRvD, 69, 063001, doi: [10.1103/PhysRevD.69.063001](https://doi.org/10.1103/PhysRevD.69.063001)
- Xu, F., Ezquiaga, J. M., & Holz, D. E. 2022, ApJ, 929, 9, doi: [10.3847/1538-4357/ac58f8](https://doi.org/10.3847/1538-4357/ac58f8)
- Xuan, Z., Naoz, S., & Chen, X. 2023, PhRvD, 107, 043009, doi: [10.1103/PhysRevD.107.043009](https://doi.org/10.1103/PhysRevD.107.043009)
- Yang, X.-Y., Chen, T., & Cai, R.-G. 2024, arXiv e-prints, arXiv:2410.16378, doi: [10.48550/arXiv.2410.16378](https://doi.org/10.48550/arXiv.2410.16378)
- Yunes, N., Miller, M. C., & Thornburg, J. 2011, PhRvD, 83, 044030, doi: [10.1103/PhysRevD.83.044030](https://doi.org/10.1103/PhysRevD.83.044030)
- Zackay, B., Venumadhav, T., Dai, L., Roulet, J., & Zaldarriaga, M. 2019, PhRvD, 100, 023007, doi: [10.1103/PhysRevD.100.023007](https://doi.org/10.1103/PhysRevD.100.023007)
- Zevin, M., Romero-Shaw, I. M., Kremer, K., Thrane, E., & Lasky, P. D. 2021a, ApJL, 921, L43, doi: [10.3847/2041-8213/ac32dc](https://doi.org/10.3847/2041-8213/ac32dc)
- Zevin, M., Samsing, J., Rodriguez, C., Haster, C.-J., & Ramirez-Ruiz, E. 2019, ApJ, 871, 91, doi: [10.3847/1538-4357/aaf6ec](https://doi.org/10.3847/1538-4357/aaf6ec)
- Zevin, M., Bavera, S. S., Berry, C. P. L., et al. 2021b, ApJ, 910, 152, doi: [10.3847/1538-4357/abe40e](https://doi.org/10.3847/1538-4357/abe40e)
- Zwick, L., Capelo, P. R., & Mayer, L. 2023, MNRAS, 521, 4645, doi: [10.1093/mnras/stad707](https://doi.org/10.1093/mnras/stad707)